Celal Bayar University Journal of Science

The Relationship Between AChE and BChE Enzymes and Alzheimer's Disease: ADME, Molecular Docking, and DFT Studies of Schiff Base-Substituted Phenylpyrimidine

Kenan Gören[1]*, Mehmet Bağlan[2], Veysel Tahiroğlu[3], Ümit Yıldıko[4]

[1,2]Kafkas University, Department of Organic Chemistry, 36000 Kars, Türkiye
[3]Şırnak University, Department of Nursing, 73000 Şırnak, Türkiye
[4]Kafkas University, Department of Bioengineering, 36000 Kars, Türkiye
* kenangoren49@gmail.com
* Orcid No: 0000-0001-5068-1762

Received: August 24, 2024
Accepted: June 3, 2025
DOI: 10.18466/cbayarfbe.1538029

Abstract

The theoretical molecular structure of Ethyl 2-(2-benzylidenehydrazinyl)-4-methyl-6-phenylpyrimidine-5-carboxylate (DHPM), a pyrimidine derivative containing the Schiff base structure, was investigated using the Gaussian 09 software program. The chemical structure and chemical reactivity of the compound were calculated using Density Functional Theory (DFT). Quantum chemical calculations were performed using DFT(B3LYP/6-311G(d,p)) and DFT(B3PW91/LANL2DZ) methods and basis sets. Using these two methods and basis sets, molecular electrostatic potential (MEP) maps of the DHPM compound were drawn. Charge transfer properties of DHPM compound were analyzed using HOMO and LUMO level energy analysis. The stability of molecules as a consequence of charge delocalization and hyperconjugative interaction was studied using NBO analysis. In this study, the relationship between Alzheimer's disease and Acetylcholinesterase (AChE) (PDB:6WUY) and Butyrylcholinesterase (BChE) (PDB: 6SAM) enzymes was evaluated by molecular docking. The molecular docking scores of in molecular docking analysis were found to be -7.76 (PDB ID: 6WUY) and -7.98 (PDB ID: 6SAM) kcal. Finally in the study, ADME analysis was performed to evaluate DHPM compound as a drug according to Lipinski's rules. As a result of the ADME analysis, we think that DHPM compound will be evaluated as a drug candidate since it complies with Lipinski's rules.

Keywords: DFT, Molecular Docking, ADME, NBO, Alzheimer, 2-(2-benzylidenehydrazinyl)-4-methyl-6-phenylpyrimidine-5-carboxylate.

1. Introduction

Schiff base compounds are the products of condensation reactions of primary amines with carbonyl compounds and were first described by Hugo Schiff in 1864. The basic structural feature of these compounds, whose general formula is RHC=N–R₁, is that they contain an azomethine group (C=N) [1]. The azomethine group largely determines the chemical reactivity and complex formation abilities of these compounds. Schiff bases play important roles in both chemical and biological systems thanks to the lone pair electron in the sp^2 hybridized orbital of the nitrogen atom in their structures [2]. This feature makes them strong chelating agents that can form complexes, especially with transition metals. In addition, the fact that Schiff bases can be easily synthesized and can be structurally modified with various functional groups has made these compounds versatile [3, 4]. In recent years, the potential of Schiff base derivatives in many areas such as bioorganic chemistry, catalysis, materials science, supramolecular chemistry, drug design and corrosion inhibitors has attracted attention [5]. In particular, Schiff bases carrying hydroxyl groups at the o-position of aromatic aldehydes show high affinity as bidentate ligands towards transition metals. However, the role played by the -N=CH- (imine) group in transamination and racemization mechanisms in biological systems increases the biological importance of these compounds [6]. In addition, the interaction of Schiff base compounds with metals via chemical adsorption and the formation of protective monolayers on

metal surfaces have made them effective corrosion inhibitors [7].

In modern chemical research, the use of theoretical calculation methods supporting experimental studies is becoming increasingly widespread [8]. In this context, quantum chemistry-based methods such as Density Functional Theory (DFT) have an important place in predicting the structural and electronic properties of molecules [9]. Unlike the Hartree–Fock theory, DFT defines electron correlation over electron density functions and provides reliable results with lower computational costs thanks to this feature [10-12]. In this study, widely used exchange-correlation functionals such as Perdew-Wang (PW91) and Lee-Yang-Parr (B3LYP) and wide basis sets such as 6-311G(d,p) were preferred in the examination of the physicochemical properties of Schiff bases [13-15].

The biological importance of Schiff base derivatives is becoming more prominent with their potential applications especially for the treatment of neurodegenerative diseases such as Alzheimer's disease (AD) [16]. AD is a serious health problem characterized by memory loss and cognitive impairment in elderly individuals and its treatment is still limited. [17]. One of the most widely accepted theories, the cholinergic hypothesis, suggests that the disease is associated with a decrease in acetylcholine levels. In this context, the development of compounds that can inhibit acetylcholine esterase (AChE) and butyrylcholine esterase (BChE) enzymes is considered as an important strategy in alleviating the symptoms of AD. The inhibitory effects of Schiff bases against these enzymes make them potential pharmacophore candidates [18, 19].

In this investigation, the Ethyl 2-(2-benzylidenehydrazinyl)-4-methyl-6-phenylpyrimidine-5-carboxylate [20] (DHPM) molecule was first drawn with GaussView 6.0 and the input file was created. Ab-initio calculations were made in the Gaussian 09 package program. DFT techniques known as hybrid functioning hybrid exchange relative We choose B3LYP and B3PW91 as the study technique. Molecular optimization and electronic characteristics have been obtained utilizing both methods and basis sets. ADME profile predictions and DFT calculations were made. DHPM molecule also complied with the drug-likeness rules and exhibited good estimated ADME characteristics. Furthermore, the interaction types and binding energies of the highly active DHPM molecule were calculated through molecular docking research. The structural and functional novelty of Schiff base-phenylpyrimidine derivatives in our study was evaluated as a result of literature review and it was determined that the synthesized compounds differed from the existing structures. Especially the unique substituent arrangement in the phenyl groups attached to the pyrimidine ring and the conjugation system formed with the Schiff base distinguish these compounds from their counterparts in the literature [21, 22].

2. Materials and Methods

Theoretical calculations of the DHPM derivative compound were carried out using the Gaussian 09 software package [23]. In order to determine the most stable conformation of the molecule in the gas phase, full geometry optimizations were performed using B3LYP/6-311G(d,p) and B3PW91/LANL2DZ method/basis set combinations within the framework of Density Functional Theory (DFT). The absence of any imaginary frequency during the optimization process confirmed that the structures are true minimum energy conformers. Mulliken atomic charge analyzes based on electron density distributions were obtained and the distribution of atomic charges on the molecule was examined in detail. The obtained charge distribution data were compared graphically using Origin 2019b (64-bit, OriginLab Corporation) software. Molecular docking analyses were performed using the Maestro Molecular Modeling platform (version 11.8) from Schrödinger [24]. Target protein structures were obtained from the Protein Data Bank (PDB) database, and PDB IDs are specified separately for each analysis title [25]. Protein structures were optimized using the Protein Preparation Wizard module to remove water molecules and non-ligand heteroatoms, complete missing atoms, and determine pH-compatible protonation states during preprocessing. The ligand structure was prepared using the LigPrep module. Docking operations were performed in the standard sensitivity (SP) mode of the Glide software, and binding scores were evaluated with GlideScore. Detailed analysis and visualization of molecule-protein interactions were performed with Discovery Studio Visualizer (BIOVIA, Dassault Systèmes) software. Within the scope of these analyses, hydrogen bonds, hydrophobic interactions, π-π stacking and van der Waals forces in the binding region were examined in detail. The pharmacokinetic properties of the compound, i.e. Absorption, Distribution, Metabolism and Excretion (ADME) profile, were evaluated using the Admetlab 2.0 (https://admetmesh.scbdd.com/) online platform [26].

3. Results and Discussion

3.1. Structure Analysis

The Gaussian 09 calculation program was optimized for the structure analysis of the DHPM compound using (B3PW91/LANL2DZ), (B3LYP/6-311G(d,p) methods and basis sets. The optimized structure was examined by two different methods for bond lengths and bond angles of the compound. The length measurements and the angles among the constituent atoms were contrasted. A quantum mechanical technique called density function theory was used to perform the computations. The fundamental principle of DFT is to use the electron

density rather than the wave function to calculate the molecule's energy [27-29]. The benefit of DFT approaches is that they incorporate electron correlations into the calculations, resulting in conclusions that are more in line with experimental findings. Method using very commonly in the DFT approach is BLYP (Becke, Lee, Yang and Parr) and the B3LYP method done by modification of BLYP. In very big nuclei, electrons close to the nucleus are considered approximately effective nuclear potentials (ECPs). For these atoms, relativistic effects are a major factor in their behavior [30]. We selected the most well-known basis set, LanL2DZ, for our computations. Table 1 lists the molecule's optimized bond length parameters, which were determined utilizing the (B3PW91/LANL2DZ), (B3LYP/6-311G(d,p) methods and basis sets. This optimization provides the molecule with the least amount of energy. Without taking energy into account, a technique is described to produce a good first approximation of the transition path between particular first and last conditions of a system. In aromatic phenyl rings, bond angles and lengths are within typical limits [31].

For B3LYP and LanL2DZ methods, the C-C bond lengths range from 1.33 to 1.51 Å, whereas the C-O bond lengths range from 1.21 to 1.34 Å. The aromatic ring's C-H lengths range from 1.08 to 1.09 Å. The range of all C-C C angles is 119°–121°. Some dihedral angles produce negative results in angle degrees when atoms are used as dihedral bonds in the Gaussian 09 software. The value of these calculated values was determined by the position and state of the atoms in the bonds. We observed that the values calculated by the B3LYP and LanL2DZ methods are consistent with each other and with the values in the literatüre [32-34].

Table 1. The DHPM molecule's theoretically calculated some bond lengths (Å) and bond angles (º).

Bond Lengths	B3LYP/ 6-311G(d,p)	B3PW91/ LANL2DZ	Bond Lengths	B3LYP/ 6-311G(d,p)	B3PW91/ LANL2DZ
C4-C7	1.48709	1.48416	C13-N19	1.28188	1.30292
C7-N12	1.33814	1.35798	C13-C37	1.46245	1.46478
C7-C8	1.40976	1.48506	C14-O16	1.34675	1.37446
C8-C14	1.49138	1.46960	C14-O15	1.21046	1.24577
C8-C9	1.41350	1.42428	C16-C21	1.44848	1.47874
C9-C17	1.50489	1.50406	C20-C21	1.51479	1.51896
C11-N12	1.32849	1.34473	N10-H30	1.01708	1.02035
C9-N10	1.32993	1.34844	C17-H29	1.08853	1.09152
C11-N18	1.37577	1.38004	C13-H36	1.09774	1.09962
N18-N19	1.34504	1.36515	C3-H24	1.08238	1.08527
Bond Angles	**B3LYP/ 6-311G(d,p)**	**B3PW91/ LANL2DZ**	**Bond Angles**	**B3LYP/ 6-311G(d,p)**	**B3PW91 LANL2DZ**
C3-C4-C7	119.40307	119.16919	N18-C19-C13	117.54989	117.88401
C5-C4-C7	121.50884	121.57326	N10-C9-C17	116.14389	116.47511
C4-C7-N12	114.89793	115.06766	O15-C14-O16	123.36433	122.57738
N10-C11-N12	127.00788	126.03830	C14-O16-C21	116.43612	117.28857
N10-C11-N18	119.67585	113.16418	O16-C21-C20	107.32920	106.82177
Planar Bond Angles	**B3LYP/ 6-311G(d,p)**	**B3PW91/ LANL2DZ**	**Planar Bond Angles**	**B3LYP/ 6-311G(d,p)**	**B3PW91/ LANL2DZ**
C5-C4-C7-N12	138.41634	141.39126	C7-N12-C11-N18	-177.82100	-177.57136
C7-C8-C9-C17	-176.60012	-176.56584	N18-N19-C13-C37	179.74438	179.75867
C14-O16-C21-C20	179.67436	179.31129	C11-N10-C9-C17	-178.57091	-178.00012
C7-C8-C14-O16	-49.21604	-50.84606	N10-C9-C8-C14	-174.21494	-173.32770

3.2. Mulliken Atomic Charges

In quantum chemical computations, mulliken atomic charge determination is a crucial parameter. Because a molecule's atomic charges have an impact on a variety of characteristics, including its electronic structure, molecular polarization, and dipole moment [35-37]. Along with displaying intramolecular charge transfer and charge distribution, it also demonstrates how electron donor and acceptor pairs form. The Mulliken atom was calculated using (B3PW91/LANL2DZ), (B3LYP/6-311G(d,p) methods and basis sets [38]. Table 2 displays further calculated Mulliken atomic charge measurements for the compound using the (B3PW91/LANL2DZ), (B3LYP/6-311G(d,p) methods and basis sets. The oxygen atom connected to the aromatic ring bears a negative charge of O15 (-0.10) and O16 (-0.32), according to the distribution of mulliken atomic charge. The aromatic ring's connected H atom has a positive charge value. It was found that there were positive and negative C atoms. Furthermore, Figure 1 provides a) Structure Optimization, b) Bond Lengths, c) Atomic Mass, and d) Mulliken Charge utilizing the DFT/B3PW91/LANL2DZ method and basis set. Using the same basis sets, the mulliken charges of a few C atoms in the DHPM molecule have been compared to the graph shown in Figure 2.

Table 2. The DHPM molecule's Mulliken Atomic Charges.

ATOMS	B3LYP/ 6-311G(d,p)	B3PW91/ LANL2DZ	ATOMS	B3LYP/ 6-311G(d,p)	B3PW91/ LANL2DZ
C2	-0.072	-0.097	**N10**	-0.391	-0.108
C3	-0.062	-0.030	**N12**	-0.363	-0.103
C4	-0.011	-0.069	**O15**	0.106	-0.236
C5	-0.090	-0.055	**O16**	-0.327	-0.287
C6	-0.083	-0.104	**N18**	-0.262	-0.315
C7	0.101	0.220	**N19**	-0.191	-0.059
C8	-0.044	-0.102	**H22**	0.106	0.227
C9	0.091	-0.154	**H23**	0.106	0.227
C11	0.243	0.300	**H24**	0.129	0.272
C13	0.060	0.139	**H25**	0.185	0.140
C17	-0.235	-0.258	**H26**	0.102	0.221
C21	-0.040	-0.021	**H27**	0.127	0.251
C37	-0.004	-0.153	**H28**	0.194	0.256
C38	-0.070	-0.033	**H29**	0.109	0.246
C39	-0.076	-0.071	**H30**	0.118	0.282
C40	-0.078	-0.096	**H31**	0.109	0.211

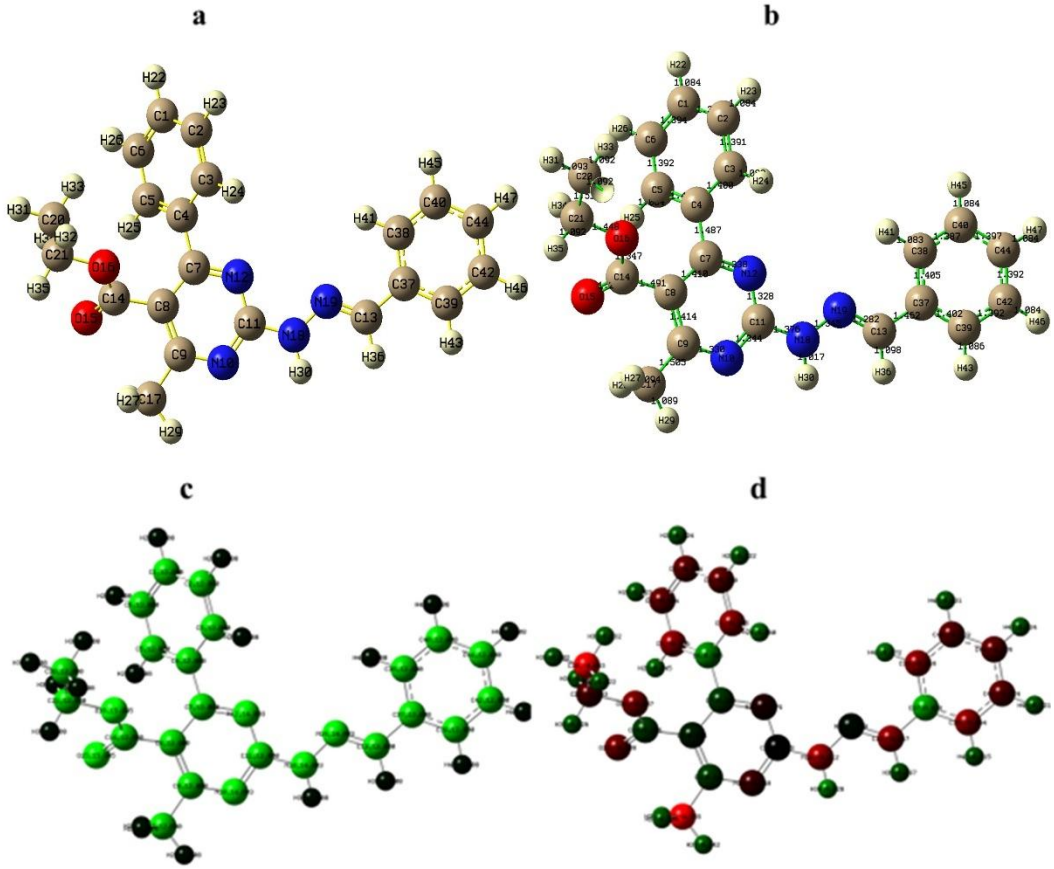

Figure 1. DHPM molecule with B3PW91/LANL2DZ method and basis set a)Structure Optimization, b)Bond Lengths, c)Atomic Mass, d)Mulliken Charge.

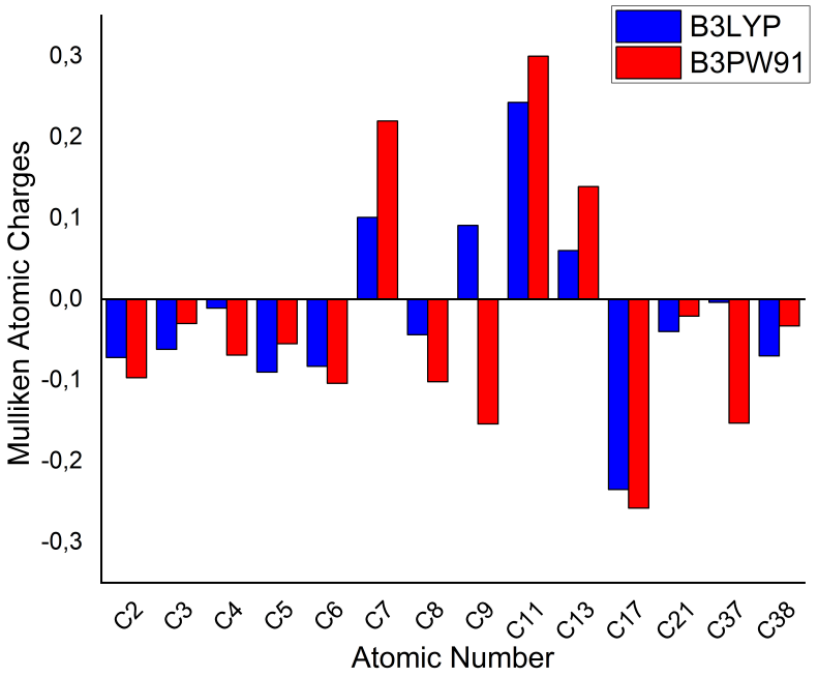

Figure 2. Mulliken atomic charge comparison for DHPM molecule.

3.3. HOMO and LUMO Analysis

In frontier molecular orbitals, HOMO denotes a wide variety of donor orbitals, while LUMO denotes acceptor orbitals [39-42]. By measuring the band gap, the lowest unoccupied molecular orbital (LUMO), and the highest occupied molecular orbital (HOMO), The molecule's basic electrical properties can be obtained. The LUMO border orbitals, which have sufficient room to receive electrons and can function as an electron acceptor, and HOMO that has the ability to donate electrons [43]. Densities of the orbital representation of the LUMO and HOMO for the DHPM molecule have been given in Figures 3 and 4. As can be observed in Table 3, the B3LYP method yielded HOMO -1.70500 eV, LUMO -5.8405 eV, whereas the LanL2DZ method yielded -2.9015 eV, -5.9553 eV respectively. For additional orbits, HOMO-1 -6.8054 eV and LUMO+1 -1.5083 eV were estimated using the B3LYP technique while HOMO-1 -6.7771 eV and LUMO+1 -1.6462 eV were calculated using the LanL2DZ method. Because characteristics like energy and molecular orbitals (HOMO-LUMO) are crucial for quantum chemistry and are particularly helpful to physicists and chemists. An electron pulse from HOMO to LUMO is identified using boundary molecular orbital analyses. The electron affinity and ionization potential are intimately correlated with the HOMO and LUMO energies, respectivel. The energy gap between the HOMO and LUMO molecules describes the possible transfer of charge during interaction [44]. Molecules possessing soft expression, strong chemical reactivity, and low kinetic stability are typically linked to their frontier orbital space. The HOMO and LUMO orbitals of the molecule control how it interacts with other molecules. Moreover, it aids in the characterization of kinetic stability, chemical reactivity, and band gap. A molecule with orbital space has polarization, hardness, electronegativity, and other reactivity indices indicated by a narrow boundary [45].

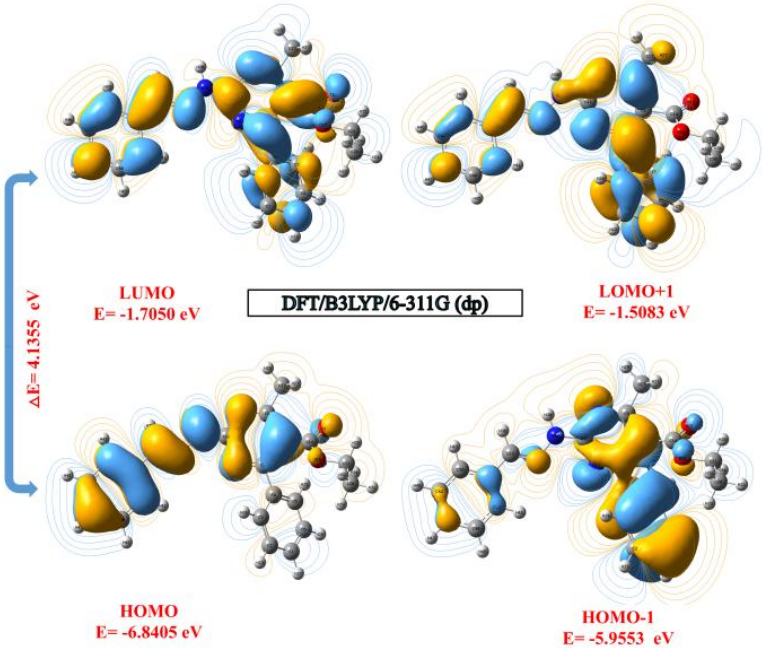

Figure 3. The DHPM molecule's boundary molecular orbitals calculated using the DFT/B3LYP/6-311G(d,p) method and basis set.

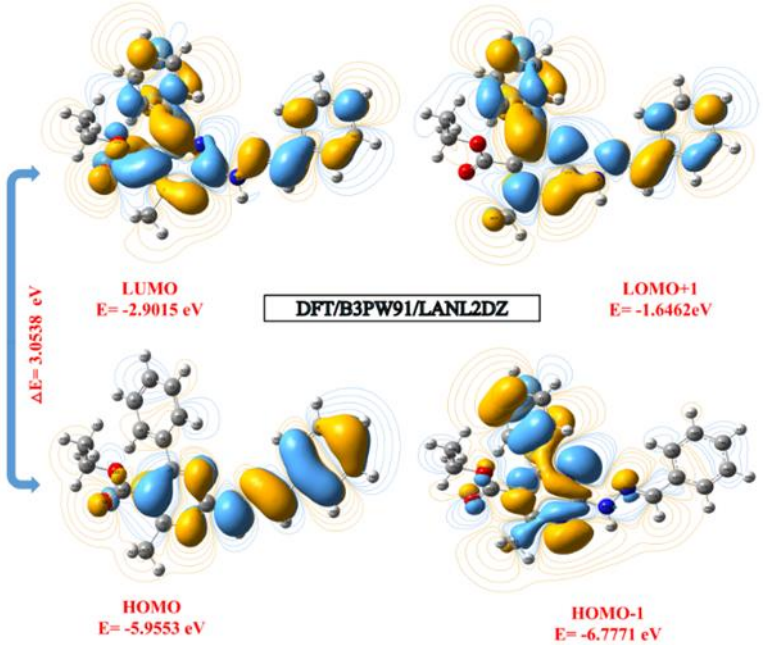

Figure 4. The DHPM molecule's boundary molecular orbitals calculated using the DFT/B3PW91/LANL2DZ method and basis set

Celal Bayar University Journal of Science
Volume 21, Issue 4, 2025, p 1-15
Doi: 10.18466/cbayarfbe.1538029

Table 3. Quantum chemical characteristics (in eV) of the DHPM molecule calculated using the B3LYP/6-311G(d,p), B3PW91/LANL2DZ methods and basis sets.

Molecules Energy		DFT/B3LYP/ 6-311G(d,p)	DFT/B3PW91/ LANL2DZ
E_{LUMO}		-1.7050	-2.9015
E_{HOMO}		-5.8405	-5.9553
E_{LUMO+1}		-1.5083	-1.6462
E_{HOMO-1}		-6.8054	-6.7771
Energy Gap	$(\Delta E)\lvert E_{HOMO}-E_{LUMO}\rvert$	4.1355	3.0538
Ionization Potential	$(I=-E_{HOMO})$	5.8405	5.9553
Electron Affinity	$(A=-E_{LUMO})$	1.7050	2.9015
Chemical hardness	$(\eta=(I-A)/2)$	2.0677	1.5269
Chemical softness	$(s=1/2\eta)$	1.0338	0.7634
Chemical Potential	$(\mu=-(I+A)/2)$	-3.7727	-4.4355
Electronegativity	$(\chi=(1+A)/2)$	1. 3525	1.7993
Electrophilicity index	$(\omega=\mu^2/2\eta)$	3.4418	-2.9015

3.4. Molecular Electrostatic Potential (MEP)

To the DHPM molecule, MEP displays the molecule's size, shape, and electrostatic potential levels. MEP map is very useful for examining the physicochemical properties of molecular structure [46]. Electrophilic assault can occur on the portion of the compound having a negative electrostatic potential [47]. In the MEP map, the blue and red areas represent electron-rich and electron-deficient regions, and correlate to negative and positive potential regions [48]. Electrostatic potential neutrality is indicated by the color green. Figure 5 illustrates how MEP was mapped for the DHPM molecule in this investigation. The DHPM molecule's MEP red spots on the map indicate the areas of negative potential surrounding the oxygen atoms. The DHPM molecule's oxygen atoms are surrounded by a much larger region known as the most negative potential zone (dark red), which allows to electrophilic interaction. The hydrogen atom (dark blue) has the highest positive charge. In Figure 5, the MEP map of the DHPM compound has been given using B3LYP/6-311G(d,p), B3PW91/LANL2DZ methods and basis sets. The difference of the order of 1×10^{-2} observed in Figure 5 is due to the difference in the level of electron correlation or basis set completeness between the methods or basis sets used. This indicates that the more advanced method or larger basis set more accurately represents the electronic structure of the system.

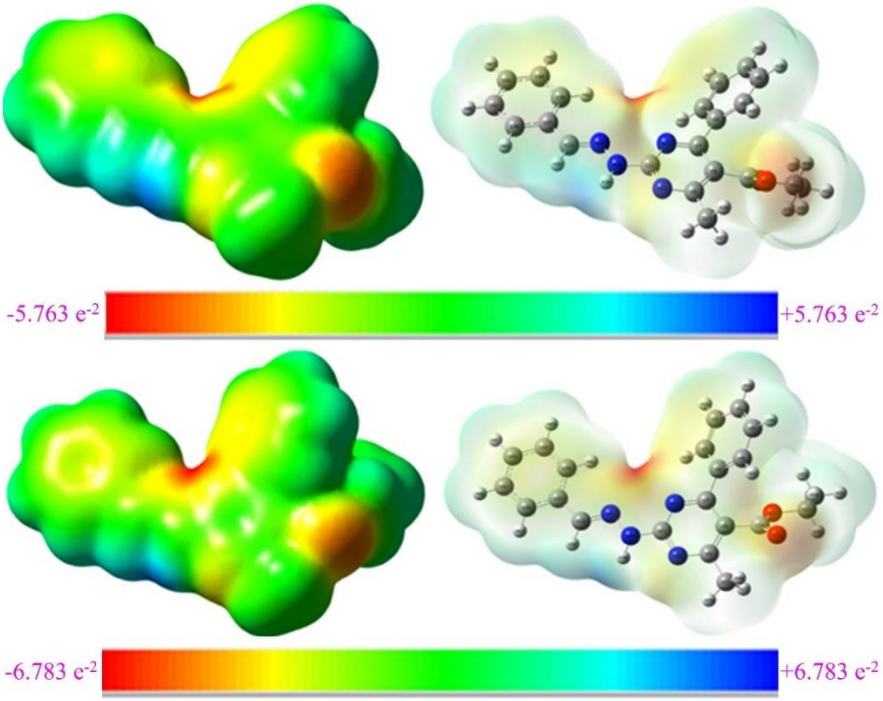

Figure 5. The DHPM molecule's MEP surface calculated using the B3LYP/6-311G(d,p), B3PW91/LANL2DZ methods and basis sets.

3.5. Non-Linear Optical Properties

One significant part of the energy connected to the electromagnetic field that is supplied to the molecule is its dipole moment. Strong intermolecular attraction is produced via intermolecular interactions involving dipole forces of the Van der Waals kind, which are the fundamental component of the dipole moment [49]. Calculated parameters, total and electronic dipole moment have been displayed in Table 4. Dipole moment's the values, hyper polarizability (β), and molecular polarization (α) are crucial in identifying the characteristics of nonlinear optics (NLO). The average values of the x, y, and z components' total first static hyperpolarizability (β), static dipole moment (μ), and polarizability (α) are provided by equations (1) through (3). The molecule's the dipole moment has a significant role in how much energy it has and is dependent upon the electrical field that it encounters [50]. Intermolecular interactions, such as Van der Waals type dipole forces, which are the essential building block of the dipole moment, result in strong intramolecular attraction. The calculated parameters and the electronic and total dipole moments have been given in Table 4. When determining the properties of nonlinear optics (NLO), dipole moment's the values, molecular polarization (α), and hyper polarizability (β) are critical.

$$\mu = \left(\mu_x^2 + \mu_y^2 + \mu_z^2\right)^{1/2} \quad (1)$$

$$\beta_{Total} = (\beta^2 x + \beta^2 y + \beta^2 z)^{1/2} \quad (2)$$

$$= [(\beta xxx + \beta xyy + \beta xzz)^2 + (\beta yyy + \beta yxx + yzz)^2 + (\beta zzz + \beta zxx + \beta zyy)^2]^{\frac{1}{2}} \quad (3)$$

Table 4. NLO parameters of DHPM molecule calculated using the B3LYP/6-311G(d,p), B3PW91/LANL2DZ methods and basis sets.

Parameters	B3LYP/ 6-311G(d,p)	B3PW91/ LANL2DZ	Parameters	B3LYP/ 6-311G(d,p)	B3PW91/ LANL2DZ
μ_x	0.5240	0.3483	β_{XXX}	50.1087	57.6438
μ_y	0.4900	0.4376	β_{YYY}	12.1062	21.3404
μ_z	1.4076	1.6523	β_{ZZZ}	2.2569	6.8492
$\mu_{(D)}$	1.5799	1.7444	β_{XYY}	16.5375	20.8044
α_{XX}	-135.0268	-129.1343	β_{XXY}	22.9464	26.4633
α_{YY}	-141.8990	-137.8042	β_{XXZ}	43.3387	57.7564
α_{ZZ}	-160.5783	-161.2633	β_{XZZ}	-40.7881	-48.3109
α_{XY}	-11.6318	-13.3959	β_{YZZ}	-6.0339	-4.7945
α_{XZ}	-3.5232	-4.3805	β_{YYZ}	5.2683	6.1840
α_{YZ}	-2.2322	-2.3206	β_{XYZ}	19.6222	22.8479
α(au)	−145.8347	−142.7339	β(esu)	5.37×10^{-31}	7.43×10^{-31}

3.6. NBO Analysis

Determining the most stable Lewis structure of the molecule and examining the detailed electron density of the orbitals is possible with Natural Bonding Orbital (NBO) analysis. The assessment of occupied and empty orbital contacts, or the NBO approach, yields data on intra- and intermolecular interactions. The quadratic Fock matrix was used in the NBO study of our chemical to assess donor-acceptor interactions [51, 52]. NBO computation explains various second-order interactions between occupied orbitals of one subsystem and unoccupied orbitals of another subsystem. These are hyperconjugation and delocalization measurements [53, 54]. In the Table 5 values comparisons utilizing the DFTB3PW91/LANL2DZ method and basis set show the percentages of individual bond electrons in various bonds as well as differences in the percentages of electrons in the s, p, and d orbitals in each atom. The relationship between the donor (i) and acceptor (j) was estimated using the Fock matrix. For each donor (i) and recipient (j), the stabilizing value associated with delocalization is expected to be as follows. NBO analysis results have been given in Table 5. Increases in electron density (ED) in antibonding orbitals are indicative of intramolecular interactions, as they weaken the pertinent bonds (C-O). More localization is provided by σ bonds since their occupancy rate is larger than that of σ* bonds. These results clearly illustrates how the intramolecular hyperconjugative interaction of the π (C2–C3) electron distribution in the ring results in the stability of portion of the ring. The intramolecular hyperconjugative interaction of π* (C1-C6) and anti π* leads to the stabilization of 22.25 kcal mol^{-1} in the Ring (C4-C5). Strong localization resulted from higher conjugation caused by these values.

Table 5. Selected NBO results of DHPM molecule calculated using B3PW91, LANL2DZ method and basis set.

NBO(i)	Type	Occupancies	NBO(j)	Type	Occupancies	E(2)[a] (Kcal/mol)	E (j)-E(i)[b] (a.u.)	F (i, j)[c] (a.u)
C1-C2	σ	1.98083	**C1-H22**	σ*	0.01536	3.24	1.20	0.056
C1-C6	π	1.98035	**C4-C5**	π*	0.36999	22.25	0.29	0.072
C1-H22	σ	1.97762	**C5-C6**	σ*	0.01547	5.17	1.07	0.067
C2-C3	π	1.64762	**C1-C6**	π*	0.33285	22.96	0.28	0.072
C2-H23	σ	1.97669	**C3-C4**	σ*	0.02545	5.52	1.06	0.068
C3-C4	σ	1.96882	**C7-C8**	σ*	0.04395	3.46	1.19	0.058
C3-H24	σ	1.97557	**C4-C5**	σ*	0.36999	6.18	1.04	0.072
C4-C5	π	1.63490	**C1-C6**	π*	0.33285	21.30	0.28	0.070
C4-C7	σ	1.96335	**C11-N12**	σ*	0.03755	5.15	1.12	0.068
C5-H25	σ	1.97387	**C3-C4**	σ*	0.02545	5.85	1.06	0.070
C6-H26	σ	1.97661	**C4-C5**	σ*	0.02612	5.67	1.05	0.069
C7-C8	σ	1.96839	**C14-O15**	π*	0.27058	0.50	0.69	0.018
C7-N12	σ	1.97545	**C11-N18**	σ*	0.04564	4.54	1.24	0.067
C8-C9	σ	1.96721	**C4-C7**	σ*	0.03797	5.18	1.16	0.069
C9-N10	π	1.74871	**C11-N12**	π*	0.45072	34.15	0.30	0.094
C9-C17	σ	1.97620	**N10-C11**	σ*	0.04043	5.51	1.08	0.069
N10-C11	σ	1.97786	**C7-C8**	π*	0.37352	31.17	0.33	0.093
C13-N19	π	1.92229	**C37-C39**	π*	0.38741	10.29	0.37	0.060
C13-H36	σ	1.98406	**C37-C38**	σ*	0.02694	5.34	1.09	0.068
C13-C37	σ	1.96723	**N18-N19**	σ*	0.02378	6.01	1.00	0.069
C14-O15	π	1.98490	**C7-C8**	π*	0.37352	2.11	0.41	0.029
C17-H28	σ	1.96995	**C9-N10**	σ*	0.02115	5.19	0.49	0.049
N18-N19	σ	1.98265	**C13-C37**	σ*	0.02572	3.33	1.35	0.060
C20-C21	σ	1.98857	**C14-O16**	σ*	0.10800	3.44	0.92	0.051
C37-C39	π	1.63512	**C13-N19**	π*	0.21063	21.95	0.24	0.068
C38-C40	π	1.66637	**C37-C39**	π*	0.38741	21.23	0.28	0.070
C42-C44	π	1.66120	**C37-C39**	π*	0.38741	21.49	0.28	0.071
C44-H47	σ	1.97777	**C38-C40**	σ*	0.01466	5.02	1.08	0.066

3.7. Molecular Docking Studies

The Protein Data Bank (http://www.rcsb.org) was used to choose the protein crystal structures of different enzymes for the chemical DHPM. The enzymes AChE (PDB ID: 6WUY) and BChE (PDB ID: 6SAM) have been employed as protein receptors. Schrodinger suite version 11.8 Maestro, a commercial program, was used for placement work [55]. As per prior research, ligand preparation and protein preparation were carried out using the LigPrep and Protein preparation modules [56, 57]. The results showed that the enzyme binding affinity was -7.76 and -7.98 kcal. We observed that the calculated docking values are compatible with each other and with the values in the literatüre [58, 59]. After determining the optimal docking conformations, protein-ligand interactions were analyzed using the Discovery Studio Client 2021 program.

Patients with Alzheimer's disease are known to experience mental, functional, and behavioral impairments as a result of diminished cholinergic activity. The cholinergic hypothesis aims to counteract this situation by increasing the neurotransmitter acetylcholine, which is decreasing in brain synapses [60]. Enzymes known as cholinesterase hydrolyze the neurotransmitter acetylcholine in the synaptic area. Acetylcholine levels rise when these cholinesterase enzymes, AChE and BChE, are inhibited. This raises cholinergic activity. Receptor agonists or cholinesterase enzyme inhibitors (ChEI) are typically used in treatments to boost the activity of the cholinergic system [61]. Currently being used as acetylcholinesterase (AChE) inhibitors in the treatment of AD, the FDA has approved the following compounds: galantamine, donepezil, tacrine, and rivastigmine. The only authorized medications in use now are these inhibitors [62]. Most studies have focused on developing inhibitors that are specific to either AChE or BChE. For example, AChE-specific inhibitors like donepezil tend to have high affinity for AChE but low binding to BChE. This study performed molecular docking studies on both 6WUY (AChE) and 6SAM (BChE) protein structures, showing that your compounds bind to both enzymes with similar binding energies [63, 64]. In order to evaluate the reliability of our docking protocol, re-docking was performed using co-crystallized ligands taken from the Protein Data Bank (PDB). For the 6WUY enzyme, the docking score was found to be 8.10 using the 4-(aminocarbonyl)-1-[({2-[(e)-(hydroxyımıno)methyl]pyridinium-1-yl}methoxy)methyl]pyridinium control ligand. Similarly, for the 6SAM enzyme, the docking score was found to be 8.30 using the [(3{s})-1-(2,3-dihydro-1{h}-inden-2-yl)piperidin-1-ium-3-yl]~{n}-phenylcarbamate control ligand. In each protein-ligand complex, the original ligand molecule was removed and then re-docked to the same binding site using the docking

protocol. The re-docked poses were compared with the original ligand positions in the crystal structures and RMSD (root mean square difference) values were calculated. The RMSD values were found to be 1.9 and this value was <2.0 Å, indicating that the protocol can reconstruct the original binding positions with high accuracy.

Table 6. Docking score of DHPM molecule PDB: 6WUY and PDB: 6SAM.

Compound	Docking Score	
	(PDB:6WUY)	(PDB:6SAM)
DHPM Molecule	-7.766	-7.980
Control Ligand	-8.102	-8.301

The 6WUY-AChE docking study's 3D and 2D interactions with the DHPM molecule have been given in Figure 6. The DHPM molecule's 6SAM-AChE binding affinity was found to be -7.76 kcal/mol. In this binding mechanism, the benzene ring is bound by the hydrogen bond HOH-807, while the phenyl pyrimidine is bound by TYR-124 (6.44 Å) conventional hydrogen bond and the oxygen is bound by PHE -295 (5.23 Å). In SER-293 (4.34 Å), a carbon hydrogen bond is formed. Pi-Alkyl is attached to phenyl pyrimidine in TYR-341 (3.94 Å) while π–π interaction was observed between the benzene ring and the molecule. This interaction occurs through weak but directional bonds between the aromatic rings. In our compound's binding mechanism, van der Waals-bonded hydrogen has been found in GLY-121, ELT-635, and ASN-87.

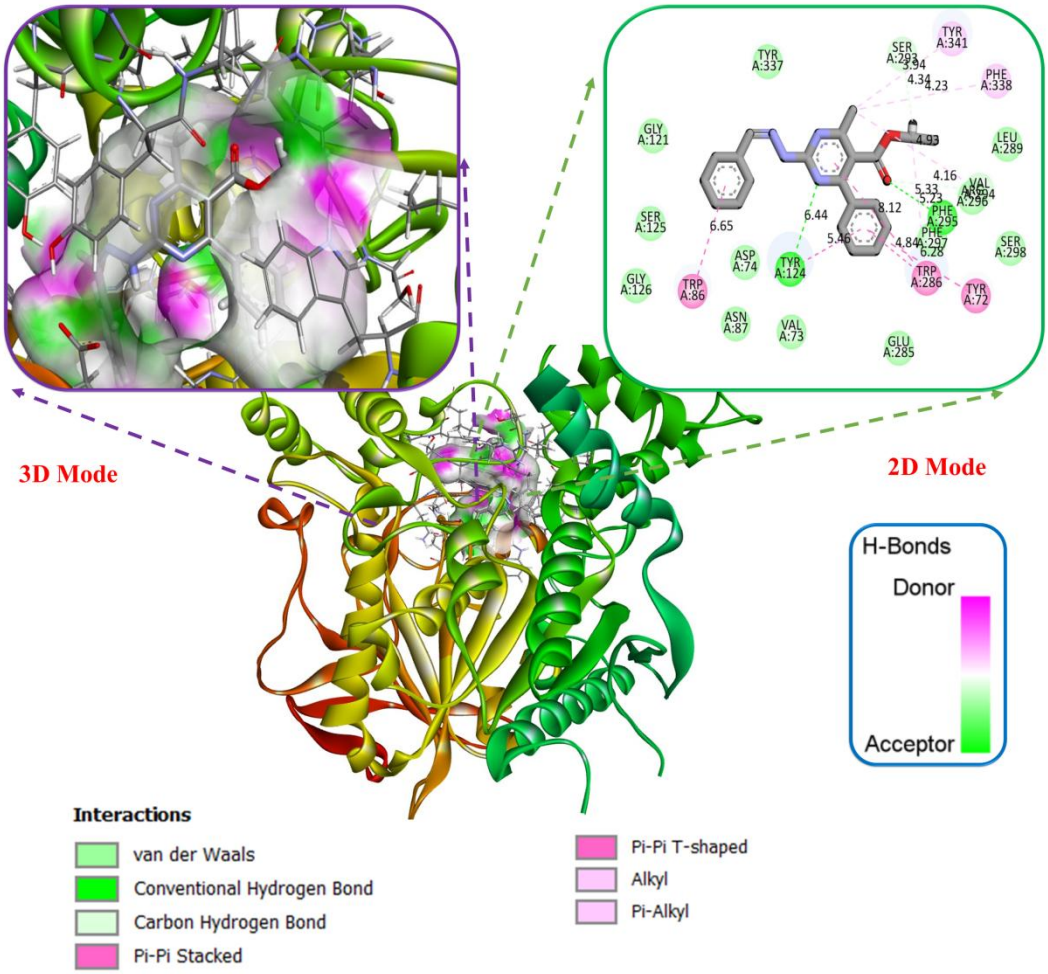

Figure 6. 3D and 2D representation of the interaction between DHPM compound and AChE enzym.

The 6SAM-BChE docking study's 3D and 2D interactions with the DHPM molecule have been given in Figure 7. The DHPM molecule had a maximum binding affinity score of -7,980 kcal/mol. Normal hydrogen bonds are bonded to nitrogen and oxygen by HIS-438 (4.38 Å) and GLY-117 (3.96 Å), while bonds to oxygen are bonded by PHE-329 (4.24 Å) and ALA-328 (4.72 Å). They are bonds of pi-alkyl. Pi-sulfur bond DMS-601

(4.97 Å) is joined to the benzene ring. The pi-donor hydrogen bond cannot form without nitrophenyl hydrogen. In our compound's binding mechanism, van der Waals-bonded hydrogen is found in GLN-119, THR-120, and ALA-277.

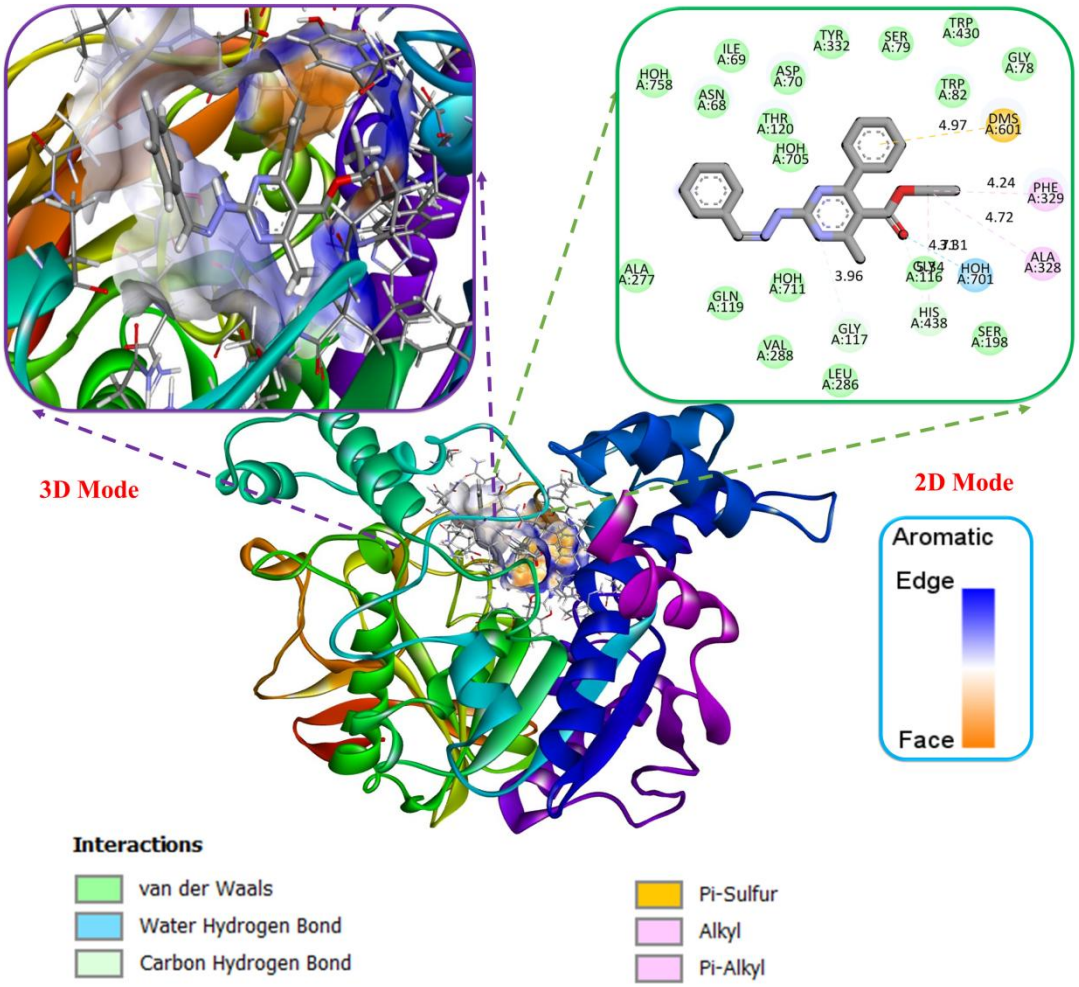

Figure 7. 3D and 2D representation of the interaction between DHPM compound and BChE enzym.

3.8. ADME Analysis

The field of computational ADME modeling is fairly developed, yet it is still evolving. Drug design commonly uses in silico ADME techniques. Additionally, the synthesized DHPM compound demonstrated appropriate predicted ADME properties and met the drug-likeness requirements [65]. An evaluation was done using SwissADME, a free online tool for determining drug-likeness properties. After this analysis, it was found to be compatible with the Lipinski (Pfizer) rules [66]. We used the web servers SwissADME (http://www.swissadme.ch/index.php) to examine this ligand molecule's biological and chemo-informatic characteristics. Table 7 shows the physicochemical and lipophilicity values obtained as a result of ADME analysis of DHPM molecule. The values obtained from the ADME analysis result; LogP values 3.81 (<10) and H-bond donor 1 (<10) Topological PSA 76.47<140 A2, MW 360.41 g/mol (<500) and ABS 82.61% were calculated and these values are compatible with Lipinski rules (values given in parentheses). Since it carries Lipinski rules, DHPM molecule can be evaluated as a drug candidate.

Table 7. Physicochemical and lipophilicity of DHPM molecule.

Code DHPM	Lipophilicity consensus log P	Physico-chemical properties								
		MW[a] g/mol	Heavy Atoms	Aromatic heavy atoms	Rot. bond	H-acceptor bond	H-donor bond	MR[b]	TPSA[c] (A^2)	% ABS[d]
	3.81	360.41	28	18	7	5	1	106.00	76.47	82.61

[a]**MW**, molecular weight; [c]**TPSA**, topological polar surface area; [b]**MR**, molar refractivity; [d]**ABS%:** absorption percent $ABS\% = 109[0.345 \times TPSA]$.

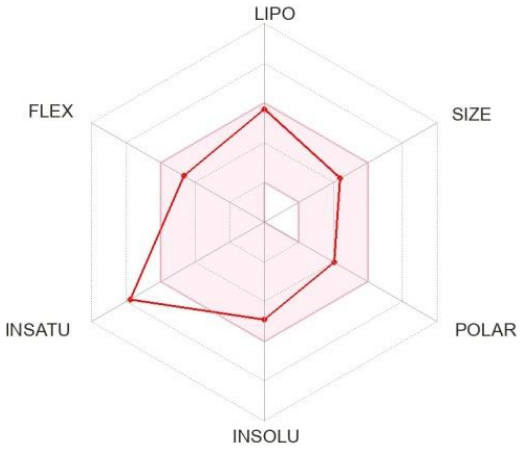

Figure 8. Color regions and physicochemical parameters of DHPM molecule.

4. Conclusion

In this study, the data obtained by theoretical and computational chemistry methods performed on Ethyl 2-(2-benzylidenehydrazinyl)-4-methyl-6-phenylpyrimidine-5-carboxylate (DHPM) compound were evaluated in detail. The structural and electronic properties of the molecule were optimized using two different density functional theory (DFT) methods, B3LYP/6-311G(d,p) and B3PW91/LANL2DZ. The obtained geometry optimization results showed that the bond lengths, bond angles and dihedral angles were compatible with both methods and gave consistent results when compared to similar structures reported in the literature. In the electronic structure analysis, HOMO and LUMO energy levels were calculated as approximately –5.84/–5.95 eV and –1.70/–2.90 eV, respectively. This low energy difference (HOMO–LUMO gap) suggests that the molecule has high chemical reactivity and may have biological activity. In the molecular electrostatic potential (MEPS) maps, the dark red regions, especially concentrated around oxygen atoms, revealed that the molecule has a high attraction power against electrophilic agents. Similarly, the high positive potential observed in the areas where hydrogen atoms are located (dark blue areas) indicate nucleophilic interaction regions. In terms of NLO (nonlinear optical) properties, the calculated polarizability and hyperpolarizability values show that the DHPM molecule has a high optical response and therefore is a potential NLO material that can be used in the field of optoelectronics in the future. Especially the high values of polarizability (α) and hyperpolarizability (β) reveal that the molecule offers significant advantages in its interaction with light. Within the scope of molecular docking analyses, the interaction of the DHPM compound with the Alzheimer's disease-related acetylcholinesterase (AChE, PDB:6WUY) and butyrylcholinesterase (BChE, PDB:6SAM) enzymes was investigated. The binding energies obtained were -7.76 and -7.98 kcal/mol, respectively, and it was determined that the molecule showed high activity against both enzymes. It was observed that the interaction with the BChE enzyme was especially stronger, indicating that DHPM may be a potential inhibitor in the treatment of Alzheimer's disease. Finally, the pharmacokinetic properties of the DHPM compound were evaluated by ADME analysis and it was found to meet Lipinski's rules. This shows that the compound has good bioavailability and is a potential drug candidate. When all these results are evaluated together, the DHPM compound exhibits both a stable and functional structure in terms of theory and a promising profile in terms of biological activity and optical properties. Therefore, if supported by further studies, it is thought that DHPM can be a building block that can be used both in the development of therapeutic agents for Alzheimer's disease and in high-tech optoelectronic applications.

Author's Contributions

Kenan Gören and Mehmet Bağlan: Prepared and wrote the draft of the article, and performed the results analysis.

Veysel Tahiroğlu and Ümit Yıldıko: Assisted in the analytical analysis of the structure, supervised the interpretation of the results, and assisted in the preparation of the draft.

.

Ethics

There are no ethical issues after the publication of this manuscript.

References

[1]. Raczuk, E, Dmochowska, B, Samaszko-Fiertek, J, Madaj, J. 2022**.** Different Schiff Bases—Structure, Importance and Classification. *Molecules,* 27(3): 787.

[2]. Berhanu, AL, Gaurav, Mohiuddin, I, Malik, AK, Aulakh, JS, Kumar, V, Kim, K-H. 2019**.** A review of the applications of Schiff bases

as optical chemical sensors. *TrAC Trends in Analytical Chemistry,* 116(74-91. https://doi.org/10.1016/j.trac.2019.04.025.

[3]. Hodnett, EM, Dunn, WJ. 1970**.** Structure-antitumor activity correlation of some Schiff bases. *Journal of Medicinal Chemistry,* 13(4): 768-770. 10.1021/jm00298a054.

[4]. Cordes, EH, Jencks, WP. 1962**.** On the Mechanism of Schiff Base Formation and Hydrolysis. *Journal of the American Chemical Society,* 84(5): 832-837. 10.1021/ja00864a031.

[5]. Metzler, CM, Cahill, A, Metzler, DE. 1980**.** Equilibriums and absorption spectra of Schiff bases. *Journal of the American Chemical Society,* 102(19): 6075-6082. 10.1021/ja00539a017.

[6]. Gupta, KC, Sutar, AK. 2008**.** Catalytic activities of Schiff base transition metal complexes. *Coordination Chemistry Reviews,* 252(12): 1420-1450. https://doi.org/10.1016/j.ccr.2007.09.005.

[7]. Sinn, E, Harris, CM. 1969**.** Schiff base metal complexes as ligands1. *Coordination Chemistry Reviews,* 4(4): 391-422. https://doi.org/10.1016/S0010-8545(00)80080-6.

[8]. Tian, X, Song, Z, Wang, B, Zhou, G. 2020**.** A Theoretical Calculation Method of Influence Radius of Settlement Based on the Slices Method in Tunnel Construction. *Mathematical Problems in Engineering,* 2020: 5804823. 10.1155/2020/5804823.

[9]. Bağlan, M, Gören, K, Çakmak, İ. 2022**.** Theoretical Investigation of ^{1}H and ^{13}C NMR Spectra of Diethanol Amine Dithiocarbamate RAFT Agent. *Journal of the Institute of Science and Technology,* 12(3): 1677-1689. 10.21597/jist.1103750.

[10]. Parlak, C, Bilge, M, Kalaycı, T, Bardakçı, B. 2011**.** DFT, FT-Raman and FT-IR investigations of 5-o-tolyl-2-pentene. *Spectrochimica Acta Part A: Molecular and Biomolecular Spectroscopy,* 79(5): 1077-1083. https://doi.org/10.1016/j.saa.2011.04.022.

[11]. Kartal, B, Tanriverdi, AA, Yildiko, U, Tekes, AT, Çakmak, I. 2024**.** Polyimide synthesis and characterizations: DFT-assisted computational studies on structural units. *Iranian Polymer Journal,* 10.1007/s13726-024-01414-6.

[12]. Yildiko, U, Tanriverdi, AA. 2021**.** Synthesis and characterization of pyromellitic dianhydride based sulfonated polyimide: Survey of structure properties with DFT and QTAIM. *Journal of Polymer Research,* 29(1): 19. 10.1007/s10965-021-02872-9.

[13]. Becke, AD. 1988**.** Density-functional exchange-energy approximation with correct asymptotic behavior. *Physical review A,* 38(6): 3098.
[14]. Lee, C, Yang, W, Parr, RG. 1988**.** Development of the Colle-Salvetti correlation-energy formula into a functional of the electron density. *Physical review B,* 37(2): 785.

[15]. Perdew, JP. 1986**.** Density-functional approximation for the correlation energy of the inhomogeneous electron gas. *Physical review B,* 33(12): 8822.

[16]. Demir, Z, Türkan, F. 2022**.** Asetilkolinesteraz ve Bütirilkolinesteraz Enzimlerinin Alzheimer Hastalığı ile İlişkisi. *Journal of the Institute of Science and Technology,* 12(4): 2386-2395. 10.21597/jist.1161271.

[17]. Lane, CA, Hardy, J, Schott, JM. 2018**.** Alzheimer's disease. *European Journal of Neurology,* 25(1): 59-70. https://doi.org/10.1111/ene.13439.

[18]. Darvesh, S. 2016**.** Butyrylcholinesterase as a Diagnostic and Therapeutic Target for Alzheimer’s Disease. *Current Alzheimer Research,* 13(10): 1173-1177.

[19]. Yildiko, Ü, Türkan, F, Tanriverdi, AA, Ata, AC, Atalar, MN, Cakmak, İ. 2021**.** Synthesis, enzymes inhibitory properties and characterization of 2- (bis (4-aminophenyl) methyl) butan-1-ol compound: Quantum simulations, and in-silico molecular docking studies. *Journal of the Indian Chemical Society,* 98(11): 100206. https://doi.org/10.1016/j.jics.2021.100206.

[20]. Liu, M, Sun, X, Zhang, J. 2017**.** Synthesis and characterization of a series of novel 2-Schiff base-substituted phenylpyrimidine. *Arabian Journal of Chemistry,* 10(2): 167-171. https://doi.org/10.1016/j.arabjc.2014.11.053.

[21]. Nayak, SG, Poojary, B. 2019**.** Synthesis of novel Schiff bases containing arylpyrimidines as promising antibacterial agents. *Heliyon,* 5(e02318. 10.1016/j.heliyon.2019.e02318.

[22]. Liu, M, Sun, X, Zhang, J. Synthesis and characterization of a series of novel 2-Schiff base-substituted phenylpyrimidine. *Arabian Journal of Chemistry,* 10(10.1016/j.arabjc.2014.11.053.

[23]. G. W. T. M.J. Frisch, HBS, G.E. Scuseria, M.A. Robb, J.R. Cheeseman, G. Scalmani, V. Barone, B. Mennucci, G.A. Petersson, H. Nakatsuji, M. Caricato, X. Li, H.P. Hratchian, A.F. Izmaylov, J. Bloino, G. Zheng, J.L. Sonnenberg, M. Hada, M. Ehara, K. Toyota, R. Fukuda, J. Hasegawa, M. Ishida, T. Nakajima, Y. Honda, O. Kitao, H. Nakai, T. Vreven, J.A. Montgomery Jr., J.E. Peralta, F. Ogliaro, M. Bearpark, J.J. Heyd, E. Brothers, K.N. Kudin, V.N. Staroverov, R. Kobayashi, J. Normand, K. Raghavachari, A. Rendell, J.C. Burant, S.S. Iyengar, J. Tomasi, M. Cossi, N. Rega, J.M. Millam, M. Klene, J.E. Knox, J.B. Cross, V. Bakken, C. Adamo, J. Jaramillo, R. Gomperts, R.E. Stratmann, O. Yazyev, A.J. Austin, R. Cammi, C. Pomelli, J.W. Ochterski, R.L. Martin, K. Morokuma, V.G. Zakrzewski, G.A. Voth, P. Salvador, J.J. Dannenberg, S. Dapprich, A.D. Daniels, Ö. Farkas, J.B. Foresman, J.V. Ortiz, J. Cioslowski, D.J. Fox, *Gaussian 09*. 2009.

[24]. Release, S, *1: Maestro, Schrodinger, LLC, New York*. 2019.

[25]. Burley, SK, Berman, HM, Bhikadiya, C, Bi, C, Chen, L, Di Costanzo, L, Christie, C, Dalenberg, K, Duarte, JM, Dutta, S. 2019**.** RCSB Protein Data Bank: biological macromolecular structures enabling research and education in fundamental biology, biomedicine, biotechnology and energy. *Nucleic acids research,* 47(D1): D464-D474.

[26]. *ADMETlab 2.0*. [cited 2024].

[27]. Bağlan, M, Gören, K, Yıldıko, Ü. 2023**.** HOMO–LUMO, NBO, NLO, MEP analysis and molecular docking using DFT calculations in DFPA molecule. *International Journal of Chemistry and Technology,* 7(1): 38-47. 10.32571/ijct.1135173

[28]. Tahiroğlu, V, Gören, K, Yıldıko, Ü, Bağlan, M. 2024**.** IInvestigation, Structural Characterization and Evaluation of the Biological Potency by Molecular Docking of Amoxicillin Analogue of a Schiff Base Molecule. *International Journal of Chemistry and Technology,* 8(2): 190-199. 10.32571/ijct.1410570.

[29]. Gören, K, Bağlan, M, Tahiroğlu, V, Yıldıko, Ü. 2024**.** Theoretical Calculations and Molecular Docking Analysis of 4-(2-(4-Bromophenyl)Hydrazineylidene)-3,5-Diphenyl-4H-Pyrazole Molecule. *Journal of Advanced Research in Natural and Applied Sciences,* 10(4): 786-802. 10.28979/jarnas.1516154.

[30]. Zhang, G, Musgrave, CB. 2007**.** Comparison of DFT Methods for Molecular Orbital Eigenvalue Calculations. *The Journal of Physical Chemistry A,* 111(8): 1554-1561. 10.1021/jp061633o.

[31]. Tsipis, CA. 2005**.** DFT study of "all-metal" aromatic compounds. *Coordination Chemistry Reviews,* 249(24): 2740-2762. https://doi.org/10.1016/j.ccr.2005.01.031.

[32]. Ersanlı, CC, Başak, S. 2024**.** Structure Elucidation of Schiff Base-Containing Compound by Quantum Chemical Methods. *International*

Scientific and Vocational Studies Journal, 8(2): 129-136. 10.47897/bilmes.1553500.

[33]. Uluçam, G, Yentürk, B. 2019. (1E,1;E)-N,N;-(hekzan-1,6-diil)bis(1-(tiyofen-2-il)metanimin) ve (1E,1;E)-N,N;-(oktan-1,8-diil)bis(1-(tiyofen-2-il)metanimin) Schiff Baz Ligantlarının Deneysel ve Teorik Karakterizasyonu. *Journal of the Institute of Science and Technology,* 9(3): 1431-1442. 10.21597/jist.500254.

[34]. Gören, K, Bağlan, M, Yıldıko, Ü. 2025. Analysis By DFT, Adme And Docking Studies Of N'-(4-Hydroxy-3-Methoxybenzylidene)Naphtho[2,3-B]Furan-2-Carbohydrazide. *Eskişehir Teknik Üniversitesi Bilim ve Teknoloji Dergisi B-Teorik Bilimler,* 13(1): 7-23. 10.20290/estubtdb.1501639.

[35]. Bağlan, M, Yıldıko, Ü, Gören, K. 2022. Computational Investigation of 5.5",7"-trihydroxy-3,7-dimethoxy-4'-4"'-O-biflavone from Flavonoids Using DFT Calculations and Molecular Docking. *Adıyaman University Journal of Science,* 12(2): 283-298. 10.37094/adyujsci.1121018.

[36]. Gören, K, Bağlan, M, Yıldıko, Ü. 2024. Antimicrobial, and Antitubercular Evaluation with ADME and Molecular Docking Studies and DFT Calculatıons of (Z)-3-((1-(5-amino-1,3,4-thiadiazol-2-yl)-2-Phenylethyl)imino)-5-nitroindolin-2-one Schiff Base. *Karadeniz Fen Bilimleri Dergisi,* 14(4): 1694-1708. 10.31466/kfbd.1423367.

[37]. Tahiroğlu, V, Gören, K, Çimen, E, Yıldıko, Ü. 2024. Moleculer Docking and Theoretical Analysis of the (E)-5-((Z)-4-methylbenzylidene)-2-(((E)-4-methylbenzylidene)hydrazineylidene)-3-phenylthiazolidin-4-one Molecule. *Bitlis Eren Üniversitesi Fen Bilimleri Dergisi,* 13(3): 659-672. 10.17798/bitlisfen.1471235.

[38]. Hratchian, HP, Parandekar, PV, Raghavachari, K, Frisch, MJ, Vreven, T. 2008. QM:QM electronic embedding using Mulliken atomic charges: Energies and analytic gradients in an ONIOM framework. *The Journal of Chemical Physics,* 128(3): 10.1063/1.2814164.

[39]. Kalaycı, T, Kınaytürk, NK, Tunalı, B. 2021. Experimental and theoretical investigations (FTIR, UV-VIS spectroscopy, HOMO-LUMO, NLO and MEP analysis) of aminothiophenol isomers. *Bulletin of the Chemical Society of Ethiopia,* 35(3): 601-614.

[40]. Yildiko, U, Tanriverdi, AA. 2022. A novel sulfonated aromatic polyimide synthesis and characterization: Energy calculations, QTAIM simulation study of the hydrated structure of one unit. *Bulletin of the Korean Chemical Society,* 43(6): 822-835. https://doi.org/10.1002/bkcs.12521.

[41]. Gören, K, Bağlan, M, Yıldıko, Ü. 2024. Melanoma Cancer Evaluation with ADME and Molecular Docking Analysis, DFT Calculations of (E)-methyl 3-(1-(4-methoxybenzyl)-2,3-dioxoindolin-5-yl)-acrylate Molecule. *Journal of the Institute of Science and Technology,* 14(3): 1186-1199. 10.21597/jist.1467666.

[42]. Gören, K, Yıldıko, Ü. 2024. Aldose Reductase Evaluation against Diabetic Complications Using ADME and Molecular Docking Studies and DFT Calculations of Spiroindoline Derivative Molecule. *Süleyman Demirel Üniversitesi Fen Bilimleri Enstitüsü Dergisi,* 28(2): 281-292. 10.19113/sdufenbed.1474689.

[43]. Bağlan, M, Yildiko, Ü, Gören, K. 2023. DFT Calculatıons cnd Molecular Docking Study In 6-(2"-Pyrrolıdınone-5"-Yl)-(-) Epıcatechın Molecule from Flavonoıds. *Eskişehir Teknik Üniversitesi Bilim ve Teknoloji Dergisi B - Teorik Bilimler,* 11(1): 43-55. 10.20290/estubtdb.1126604.

[44]. Muthu, S, Uma Maheswari, J. 2012. Quantum mechanical study and spectroscopic (FT-IR, FT-Raman, 13C, 1H, UV) study, first order hyperpolarizability, NBO analysis, HOMO and LUMO analysis of 4-[(4-aminobenzene) sulfonyl] aniline by ab initio HF and density functional method. *Spectrochimica Acta Part A: Molecular and Biomolecular Spectroscopy,* 92(154-163. https://doi.org/10.1016/j.saa.2012.02.056.

[45]. Karabacak, M, Bilgili, S, Atac, A. 2015. Molecular structure, spectroscopic characterization, HOMO and LUMO analysis of 3,3′-diaminobenzidine with DFT quantum chemical calculations. *Spectrochimica Acta Part A: Molecular and Biomolecular Spectroscopy,* 150(83-93. https://doi.org/10.1016/j.saa.2015.05.013.

[46]. Bağlan, M, Gören, K, Yildiko, Ü. 2023. DFT Computations and Molecular Docking Studies of 3-(6-(3-aminophenyl)thiazolo[1,2,4]triazol-2-yl)-2H-chromen-2-one(ATTC) Molecule. *Hittite Journal of Science and Engineering,* 10(1): 11-19. 10.17350/HJSE19030000286.

[47]. Aydoğdu, Ö, Öztürkkan, FE, Hökelek, T, Uğurlu, G, Necefoğlu, H. 2025. Syntheses, crystal structures, and DFT calculations of N'-(Pyridin-2-ylmethylene)nicotinohydrazide dihydrate and its copper complex. *Journal of the Iranian Chemical Society,* 22(4): 683-697. 10.1007/s13738-025-03177-0.

[48]. Aydoğdu, Ö, Uğurlu, G, Necefoğlu, H, Öztürkkan, FE, Hökelek, T. 2024. Syntheses, Crystal Structure and Theoretical Properties of Schiff Bases Obtained from Isoniazid and Pyridine-2-, 3-, 4-Carboxaldehyde and Their Zinc (II) Complexes. *ChemistrySelect,* 9(14): e202304861.

[49]. Abdel Aziz, AA, Elantabli, FM, Moustafa, H, El-Medani, SM. 2017. Spectroscopic, DNA binding ability, biological activity, DFT calculations and non linear optical properties (NLO) of novel Co(II), Cu(II), Zn(II), Cd(II) and Hg(II) complexes with ONS Schiff base. *Journal of Molecular Structure,* 1141(563-576. https://doi.org/10.1016/j.molstruc.2017.03.081.

[50]. Mahmood, A, Khan, SU-D, Rana, UA, Janjua, MRSA, Tahir, MH, Nazar, MF, Song, Y. 2015. Effect of thiophene rings on UV/visible spectra and non-linear optical (NLO) properties of triphenylamine based dyes: a quantum chemical perspective. *Journal of Physical Organic Chemistry,* 28(6): 418-422. https://doi.org/10.1002/poc.3427.

[51]. Glendening, ED, Landis, CR, Weinhold, F. 2013. NBO 6.0: Natural bond orbital analysis program. *Journal of Computational Chemistry,* 34(16): 1429-1437. https://doi.org/10.1002/jcc.23266.

[52]. Kurt, M, Babu, PC, Sundaraganesan, N, Cinar, M, Karabacak, M. 2011. Molecular structure, vibrational, UV and NBO analysis of 4-chloro-7-nitrobenzofurazan by DFT calculations. *Spectrochimica Acta Part A: Molecular and Biomolecular Spectroscopy,* 79(5): 1162-1170. https://doi.org/10.1016/j.saa.2011.04.037.

[53]. Govindarajan, M, Karabacak, M. 2012. Spectroscopic properties, NLO, HOMO–LUMO and NBO analysis of 2,5-Lutidine. *Spectrochimica Acta Part A: Molecular and Biomolecular Spectroscopy,* 96: 421-435. https://doi.org/10.1016/j.saa.2012.05.067.

[54]. Gören, K, Bağlan, M, Yıldıko, Ü, Tahiroğlu, V. Molecular Docking and DFT Analysis of Thiazolidinone-Bis Schiff Base for anti-Cancer and anti-Urease Activity. *Journal of the Institute of Science and Technology,* 14(2): 822-834.

[55]. Vijesh, AM, Isloor, AM, Telkar, S, Arulmoli, T, Fun, H-K. 2013. Molecular docking studies of some new imidazole derivatives for antimicrobial properties. *Arabian Journal of Chemistry,* 6(2): 197-204. https://doi.org/10.1016/j.arabjc.2011.10.007.

[56]. Yuriev, E, Ramsland, PA. 2013. Latest developments in molecular docking: 2010–2011 in review. *Journal of Molecular Recognition,* 26(5): 215-239. https://doi.org/10.1002/jmr.2266.

[57]. Abdullah, Tanriverdi, AA, Khan, AA, Lee, S-J, Park, JB, Kim, YS, Yildiko, U, Min, K, Alam, M. 2024. Selenium-substituted conjugated small molecule: Synthesis, spectroscopic, computational studies, antioxidant activity, and molecular docking. *Journal of Molecular Structure,* 1304: 137694. https://doi.org/10.1016/j.molstruc.2024.137694.

[58]. Luedtke, S, Bojo, C, Li, Y, Luna, E, Pomar, B, Radić, Z. 2021**.** Backbone Conformation Shifts in X-ray Structures of Human Acetylcholinesterase upon Covalent Organophosphate Inhibition. *Crystals,* 11(11): 1270.

[59]. Miličević, A, Šinko, G. 2022**.** Evaluation of the Key Structural Features of Various Butyrylcholinesterase Inhibitors Using Simple Molecular Descriptors. *Molecules,* 27(20): 6894.

[60]. Arendt, T, Brückner, MK, Lange, M, Bigl, V. 1992**.** Changes in acetylcholinesterase and butyrylcholinesterase in Alzheimer's disease resemble embryonic development—A study of molecular forms. *Neurochemistry International,* 21(3): 381-396. https://doi.org/10.1016/0197-0186(92)90189-X.

[61]. Ali, B, M.S. Jamal, Q, Shams, S, A. Al-Wabel, N, U. Siddiqui, M, A. Alzohairy, M, A. Al Karaawi, M, Kumar Kesari, K, Mushtaq, G, A. Kamal, M. 2016**.** In Silico Analysis of Green Tea Polyphenols as Inhibitors of AChE and BChE Enzymes in Alzheimer’s Disease Treatment. *CNS & Neurological Disorders - Drug Targets-CNS & Neurological Disorders),* 15(5): 624-628.

[62]. Greig, NH, Lahiri, DK, Sambamurti, K. 2002**.** Butyrylcholinesterase: An Important New Target in Alzheimer's Disease Therapy. *International Psychogeriatrics,* 14(S1): 77-91. 10.1017/S1041610203008676.

[63]. Greig, NH, Utsuki, T, Yu, Q-s, Zhu, X, Holloway, HW, Perry, T, Lee, B, Ingram, DK, Lahiri, DK. 2001**.** A new therapeutic target in Alzheimer's disease treatment: attention to butyrylcholinesterase. *Current medical research and opinion,* 17(3): 159-165.

[64]. Carmona, P, Toledano Gasca, A, Álvarez-Vicente, MI, Fuiz, S, Molina, M, Calero Lara, M, Martínez-Martín, P, Bermejo Pareja, F. 2011**.** Infrared spectroscopic analysis of blood as a diagnostic tool in Alzheimer disease.

[65]. Kassel, DB. 2004**.** Applications of high-throughput ADME in drug discovery. *Current Opinion in Chemical Biology,* 8(3): 339-345. https://doi.org/10.1016/j.cbpa.2004.04.015.

[66]. Shou, WZ. 2020**.** Current status and future directions of high-throughput ADME screening in drug discovery. *Journal of Pharmaceutical Analysis,* 10(3): 201-208. https://doi.org/10.1016/j.jpha.2020.05.004